# Experiments and Large Eddy Simulations on Particle Interaction with a Turbulent Air Jet Impacting a Wall

Syphax Ikardouchene[1,2], Xavier Nicolas[1(✉)] , Stéphane Delaby[2], and Meryem Ould-Rouiss[1]

[1] Université Paris Est Marne-la-Vallée, MSME UMR 8208 CNRS,
5 Bd Descartes, 77454 Marne-la-Vallée Cedex 2, France
`Xavier.Nicolas@u-pem.fr`
[2] CSTB, 24 rue Joseph Fourier, 38400 Saint-Martin-d'Hères, France

**Abstract.** Experiments and large eddy simulations are carried out to study the interaction of spherical particles with a turbulent air jet impacting a wall. The context is that of the dynamical air curtains used to separate a contaminated ambiance with passive or inertial particles from a clean ambiance. In the present study, the jet and particle Reynolds numbers and the jet and turbulence Stokes numbers are respectively equal to $Re_j = 13500$, $0.7 \leq Re_p \leq 3.5$, $0.02 \leq St_j \leq 0.35$ and $0.1 \leq St_t \leq 1$: they mainly concern passive particles. The rate of the particles that cross the air jet is analyzed according to the particle size, for two particle injection heights. A non-monotonic passing rate of the particles through the jet with respect to the particle size is observed in the experiments.

**Keywords:** Impacting plane jet · Air curtain · Particle/jet interaction · Passive particles · Experiments · LES

## 1 Introduction

Plane air jets are widely used in industry and cover a large range of applications: cooling and wiping of liquid films by plane turbulent jets [1], spread reduction of fumes and gaseous pollutants in tunnel fires [2] etc. In our case, a plane air jet is used for the separation of two clean and polluted atmospheres by inertial and passive (non-inertial) particles. The purpose of this work is to define if large eddy simulations (LES) allow qualitatively and quantitatively reproducing the interaction between particles and a turbulent vertical air jet. In that aim, an experimental apparatus and a numerical tool based on the coupling of LES and a Lagrangian model for the particle transport have been developed. The studied configuration is that of an air jet impacting a wall (similar to that of experiments [3] and LES [4]) and crossed by particles. The objective is to study the jet dynamics without particle and, then, to inject particles towards the jet, to measure their passage rate through the jet and to compare it with that of the LES.

# 2   Analysis of the Impinging Plane Air Jet, Without Particle

## 2.1   Experimental Facility and Method

In order to characterize impacting plane air jets, we designed the experimental device of Fig. 1. A vertical plane air jet is generated by a centrifugal fan that blows air through a divergent and convergent channel, then through a rectangular nozzle of section width $e = 3$ mm in $x$-direction and depth $d_z = 200$ mm in $z$-direction. The nozzle aspect ratio $d_z/e = 66$ ensures that the flow is statistically two-dimensional and free from the side wall effects when taking measurements in the central plane ($z = 0$) of the jet. The nozzle outlet is located in the middle of the top wall of a horizontal rectangular channel of height $H = 3$ cm, depth $d_z = 200$ mm and length $L_x = 60$ cm in $x$-direction (30 cm on each side of the jet). The jet average velocity at nozzle outlet is $U_j = 65$ m/s. The jet Reynolds number $Re = U_j e/\nu = 13500$ and the opening ratio $H/e = 10$ are fixed in all the study. The analysis of the velocity field is carried out by particle image velocimetry (PIV), by seeding with oil particle tracers directly at the fan level and using a Nd-Yag laser (65 mJ, 15 Hz) and a fast camera (FS EO 4M-32).
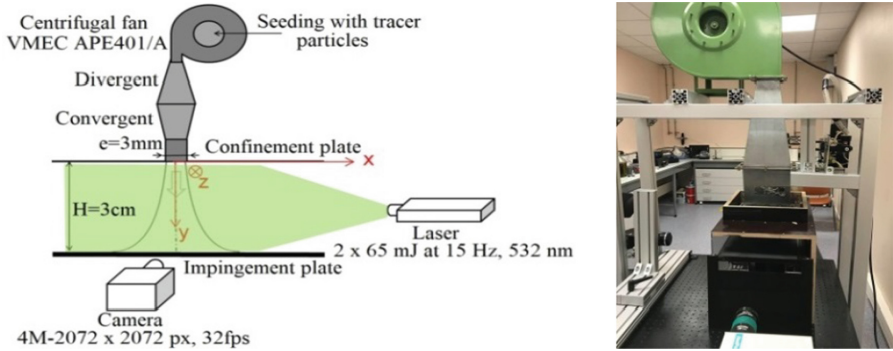


**Fig. 1.** Sketch and photography of the experimental facility.

## 2.2   Flow Configuration, LES Model and Numerical Methods

The LES are performed with the CFD code Ansys/Fluent v18.2 using the WALE model for the sub-grid effects. The filtered Navier-Stokes equations are solved by a finite volume method with a second order bounded central scheme, a second order time implicit scheme and PISO algorithm. The numerical configuration is close to that of the experiments. The computational domain size is $L_x \times L_y(H) \times L_z = 243 \times 30 \times 18.84$ mm$^3$ in the horizontal, vertical and depth directions respectively (Fig. 2 left). The vertical plane jet is injected into the

domain by a nozzle of section $L_z \times e = 18.84 \times 3\,\text{mm}^2$ located in the center of the upper horizontal wall. The experimental velocity profile measured in [3] at the outlet of the nozzle and taken up in the LES [4] is interpolated and imposed as inlet boundary conditions (B.C.) in our simulations with the average velocity $U_j = 65\,\text{m/s}$. Turbulent fluctuations in the inlet velocity profiles are generated, with a turbulent intensity $I = 2\%$, by a «spectral synthesizer». No slip B.C. are imposed on the horizontal walls and periodic B.C. on the front and back faces. The depth $L_z/e = 2\pi$ is chosen so that the time signals are decorrelated in $z$-direction [4]. The air jet impacts the lower wall and horizontally flows out through the left and right vertical openings considered at atmospheric pressure. A non-uniform Cartesian mesh of size $N_x \times N_y \times N_z = 236 \times 150 \times 64$ cells ($y^+_{max} < 5.6$) is used (Fig. 2 right). It is uniform in $z$-direction. The time step is $\Delta t = 10^{-6}$ $s$ such that $CFL_{max} = (U\Delta t/\Delta x)_{max} = 7$. The time duration for the statistics is $0.02\,\text{s}$.
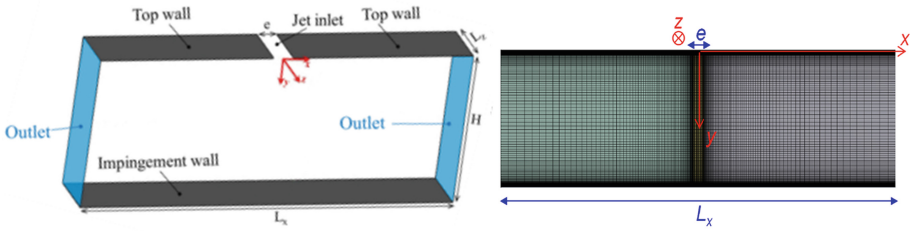


**Fig. 2.** Sketch of the computational domain (left) and mesh in the $(x-y)$ plane (right).

### 2.3   Result Discussion for an Air Jet Without Particle

Figure 3 shows average and rms velocity profiles obtained by the present PIV and LES, compared with experimental [3,5] and LES [4] results. Other validations were carried out by comparing various vertical and transverse profiles of the time averages and rms of the velocity components and pressure, the Reynolds stresses, the half width of the jet and the spectral analysis of time signals. All these results are in good agreement with the results published in the reference literature (see [6] for more details about the validations).

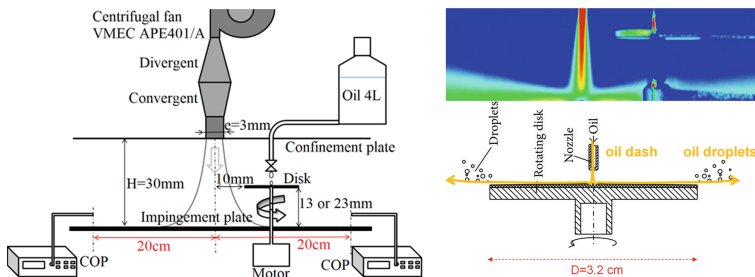## 3   Analysis of the Jet/Particles Interaction

### 3.1   Experimental Facility and Particle Generation (Spinning Disk)

To generate particles, the spinning disk method is used (Fig. 4 right). The principle is the fragmentation and dispersion of oil droplets under the centrifugal force of a rotating disk. The edge of this disk is placed at $1\,\text{cm}$ from the jet
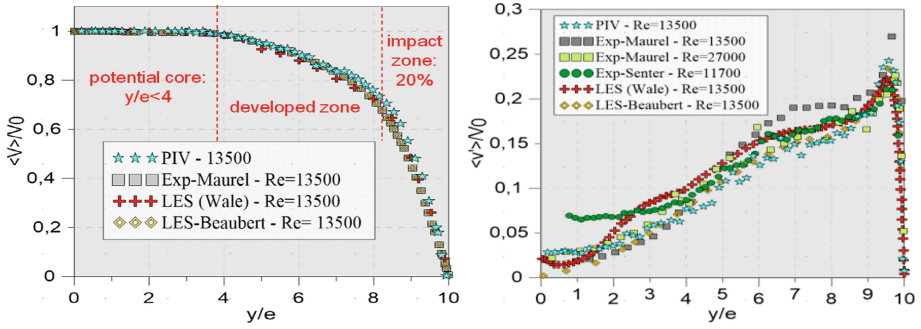
**Fig. 3.** Mean velocity magnitude (left) and vertical velocity rms (right) along jet axis.

axis and its tangential speed is $V_t = R\omega = 38\,\mathrm{m/s}$ with $R = 1.6\,\mathrm{cm}$. Figures 4 and 5 show that the presence of the rotating disk does not perturb the air jet flow. The oil mass flow rate for particle generation is $\dot{m} = 0.2\,\mathrm{g/min}$ and the generated particle diameter is $0.3 \leq d_p \leq 7\,\mathrm{\mu m}$. The particle total concentrations, $C_{p,l}$ and $C_{p,r}$, and size distribution are locally measured on the two sides of the jet, at $x = \pm 20\,\mathrm{cm}$, by an optical particle counter (COP-GRIMM; Fig. 4 left). $C_{p,l}$ is measured on the left side (opposite side of the rotating disk with respect to the jet) and $C_{p,r}$ on the right side (on the side of the rotating disk). We have checked that these concentrations are quasi homogeneous in all the channel section at this distance. The particle passing rate through the jet, defined by $PPR = \frac{C_{p,l}}{C_{p,l}+C_{p,r}}$, is computed from the average values of the concentrations measured during a ten minute particle injection in the presence of the jet, for two positions of the rotating disk: at $y = 7\,\mathrm{mm}$ (jet potential cone level) and $y = 17\,\mathrm{mm}$ (jet developed zone; Fig. 3 left). Since, the optical counter can measure the diameter $d_p$ of each particle, the $PPR$ can also be measured for each class of particle size.



**Fig. 4.** Experimental facility for the jet/particle interaction study (left). Spinning disk principle and PIV field of the mean velocity magnitude with the rotating disk (right).
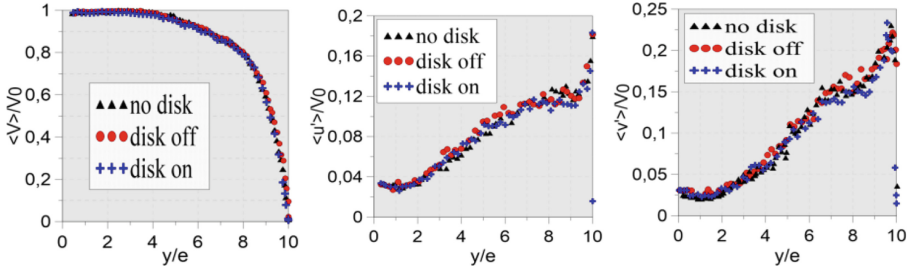
**Fig. 5.** Profiles of the mean vertical velocity (left) and rms of the horizontal (center) and vertical (right) velocities along the jet axis, with and without the disk in rotation.

### 3.2  Configuration and Parameters of the Jet/Particle Simulations

A Lagrangian model expressing the balance between the inertial, drag and gravity forces is used for the transport of the oil droplets considered as spheres. In this model, the particle relaxation time $t_p = \frac{\rho_p d_p^2}{18\mu} \frac{24}{C_D Re_p}$ and the drag coefficient $C_D = a_1 + \frac{a_2}{Re_p} + \frac{a_3}{Re_p^2}$ ($a_i = cst$) are function of $Re_p = \frac{\rho d_p |u_p - u|}{\mu}$, the particle Reynolds number. A "stochastic tracking model" is also activated in Ansys/Fluent to take into account the turbulent dispersion of the particles (see [7] for more details). Since the largest particle volume fraction was estimated around $10^{-3}$ in the spinning disk neighborhood at the end of the injection period, a two-way-coupling model was used in the simulations. Furthermore, $t_s = e/(2u_p)$ being the characteristic time of the particles to go through the half of the jet thickness and $t_\kappa$ being the Kolmogorov time scale, the jet and turbulence Stokes numbers are estimated to vary in the ranges $0.02 \leq St_j = t_p/t_s \leq 0.35$ and $0.1 \leq St_t = t_p/t_\kappa \leq 1$ (to 7, locally), when $d_p$ varies between 1 and $5\,\mu$m. Therefore the particles are mainly passive, that is with little inertial effects.

The injection and boundary conditions for the particles are presented on Fig. 6 (left). Around 1 million of spherical particles of the same diameter ($d_p = 1$, 3 or $5\,\mu$m) and density $\rho_p = 920\,\text{kg/m}^3$ are injected in the domain from a thin surface of depth $\times$ height $= 18.8 \times 1\,\text{mm}^2$, located at $x = 10\,\text{mm}$ from the air jet median plane and at $y = 7$ or $17\,\text{mm}$ from the top wall. They are injected during $2\,\text{ms}$, with a horizontal velocity $u_p = -10\,\text{m/s}$ and mass flow rate $\dot{m} = 0.3\,\text{g/min}$. Their trajectories are followed during $5\,\text{ms}$ for the injection at $y = 7\,\text{mm}$ and during $50\,\text{ms}$ at $y = 17\,\text{mm}$. The particles are reflected on the top wall and on the bottom wall in front of the air jet nozzle, but they are trapped on the rest of the bottom wall. Due to the simulation cost, the $PPR$ is only computed for the injection at $y = 17\,\text{mm}$: it is the proportion of particles of the same diameter that have passed through the jet median plane (x$=0$) at $t = 50\,\text{ms}$. The total user time of these simulations is around two months on 20-cores of recent high-performance computing workstations.
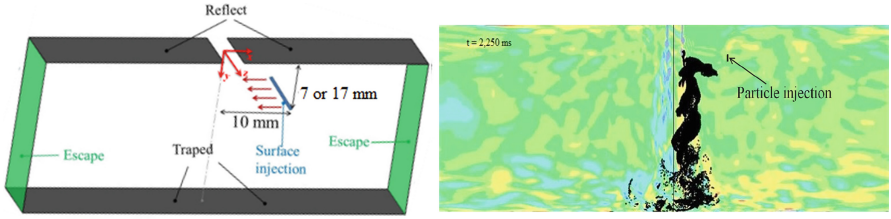
**Fig. 6.** Simulation domain with the injection line and the particle B.C. (left). Vorticity contours and $3\,\mu$m-particle location (black points) in the vertical median plane at $z = 0$, at $t = 2.25\,$ms, for the particles injected at $y = 7\,$mm from the top wall (right).

### 3.3    Result Discussion for an Air Jet with Particle Injection

Figure 6 (right) shows the particle/vorticity interaction, for $d_p = 3\,\mu$m and the injection position at $y = 7\,$mm, just after the injection period, at $t = 2.25\,$ms. The particles are driven by Kelvin Helmholtz rolls that are partially responsible for the passage of the particles through the jet, mainly in the impact zone (see also [4]). Note that, due to the presence of two large vortices on both sides of the jet (not shown here; see [6] for more details), the evacuated particles towards the channel outlets can be taken back to the jet by these vortices, for $t > 10\,$ms. This explains why the $PPR$ is measured at $t = 50\,$ms in the simulations.

The experimental time evolution of the particle concentration $C_{p,l}$ is shown on Fig. 7 (left) for three different tests. There are four distinct phases in this graph which correspond to the time variation of $C_{p,l}$: (1) in the environment (before particle injection) in order to subtract it from the following measurements; (2) with particle injection but without air jet; (3) with particle injection and with air jet (it is therefore the concentration of particles passing through the jet); (4) after stopping the particle generation. One can see that the repeatability of the measurements is ensured and a decrease in the particle concentration is observed in the presence of the jet.
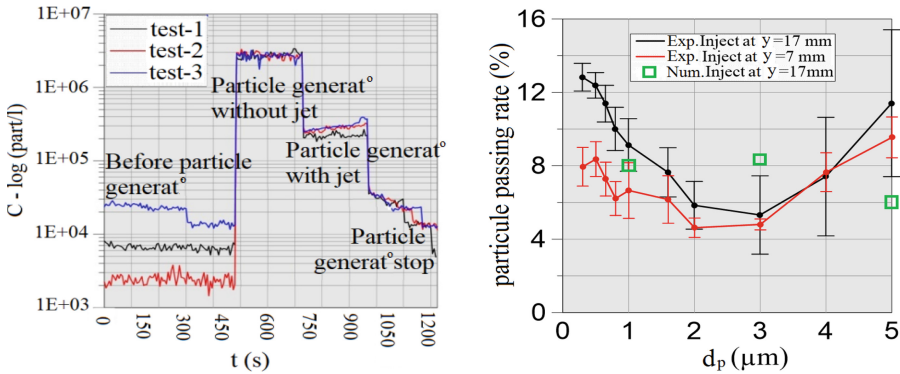


**Fig. 7.** Time evolution of the particle concentration $C_{p,l}$ (left). Passing rate of the particles through the jet with respect to the particle diameter (right).

Figure 7 (right) presents the $PPR$ evolution, for each class of particle size, with respect to $d_p$, for the two positions of the rotating disk in the experiments and at $y = 17\,\text{mm}$ for the simulations. The experimental $PPR$ values are similar for the two injection locations, except at $d_p < 1\,\mu\text{m}$. As already noted above, this can be partly explained by the presence of the two large vortices on both sides of the jet that "recycle" the particles [6]. For the injection at $17\,\text{mm}$, the experimental and numerical $PPR$ values are in a relatively good agreement when the standard deviations of the experimental results are taken into account. However a non-monotonic $PPR$ evolution with $d_p$ is clearly visible in the experiments but is not reproduced by LES. In the experiments, the larger value of the $PPR$ for the smallest $d_p$ could be due to the turbulent dispersion of the smallest particles while its increase for the largest $d_p$ could be due to inertial effects relatively to the turbulence scale ($St_{t,max} = 7$ for $d_p = 5\,\mu\text{m}$). This small-scale phenomenon is filtered by LES and likely not taken into account in the numerical model. Another explanation could be the coalescence (resp., the break-up) of the oil droplets, increasing then the $PPR$ of the biggest (resp., smallest) particles.

## 4    Conclusions

In the first part of this study, an analysis of the air jet dynamics without particles has been performed with PIV and LES simulations. The comparison of the results has shown that the Wale LES model is appropriate to simulate a turbulent air jet impacting a wall. In the second part, the interactions between this air jet and spherical particles of different diameters was investigated by the two approaches. The method of particle generation by a spinning disk has appeared to be a very interesting method because it does not perturb the jet. The experiments have enabled to set up reference results to validate simulations with particle/jet interaction because no experiment exists in the literature for this configuration. The LES have enabled a better understanding of the particle/jet interactions, in particular the interactions with the Kelvin-Helmholtz rolls. A non-monotonic passing rate of the particles through the jet with respect to the particle size has been experimentally observed. This paper is a presentation of the first results of this study but new results and deeper analyses are in progress.

## References

1. Lacanette, D., Vincent, S., Arquis, E.: A numerical experiment on the interaction between a film and a turbulent jet. Comptes Rendus Mécanique **333**, 343–349 (2005)
2. Guyonnaud, L., Solliec, C., Dufresne de Virel, M., Rey, C.: Design of air curtains used for area confinement in tunnels. Exp. Fluids **28**(4), 377–384 (2000)
3. Maurel, S., Solliec, C.: A turbulent plane jet impinging nearby and far from a flat plate. Exp. Fluids **31**(6), 687–696 (2001)

4. Beaubert, F., Viazzo, S.: Large eddy simulation of plane turbulent impinging jets at moderate Reynolds numbers. Int. J. Heat Fluid Flow **24**, 512–519 (2003)
5. Senter, J.: Analyse expérimentale et numérique des écoulements et des transferts de chaleur convectifs produits par un jet plan impactant une plaque plane mobile. Ph.D. thesis, Univ. de Nantes (2006)
6. Ikardouchene, S.: Analyses expérimentale et numérique de l'interaction de particules avec un jet d'air plan impactant une surface. Application au confinement particulaire. Ph.D. thesis, Univ. Paris Est (2019)
7. ANSYS Fluent Theory Guide, Release 17.2. Ansys Inc., Canonsburg (2016)